IAA-AAS-DyCoSS2-13-05

The Detection and Identification of Control Moment Gyro Faults

Hwa-Suk Oh[*] and Ji-Chul Kim[†]

When control moment gyros (CMGs) are employed as satellite actuators, they generate a large amount of torque through the steering of their gimbals. Each gimbal holds a high speed rotating wheel. Wheel speed error and imbalances induce disturbances and degrade satellite control quality. Disturbances thus need to be detected and identified as a precaution against actuator faults. State observers have been used as one method of detecting disturbances. A continuous second order sliding mode observer is suggested and applied for the detection of single disturbances/faults on CMGs. A frequency compensation algorithm is also suggested for the improvement of magnitude identification on the existence of highly oscillating disturbances. Highly oscillating disturbances induced by wheel speed errors and imbalance faults are thus satisfactorily detected and identified even in the high frequency domain.

INTRODUCTION

Among various momentum exchanging actuators, control moment gyros (CMGs) have been used as primary attitude control actuators for a variety of spacecraft. Slew or reorientation maneuvers are executed by exchanging their angular momentum with that of a spacecraft body.[1] The wheel momentum variation provides the spacecraft with maneuvering capability – the control torque. However, the vibrational force and torque disturbances induced by CMG faults such as as wheel bearing wear, misalignment, and severe wheel speed fluctuations degrade the attitude quality of the spacecraft.[2-4] Severe faults in actuators need to be detected and isolated in real time in orbit.

Model-based observers are one fault detection and isolation (FDI) method. They rely mainly on system dynamic models.[5] Since a spacecraft model is intrinsically nonlinear in a large angle maneuver, a proper nonlinear FDI approach should be adopted.[6,7] A nonlinear sliding mode observer (SMO) can be used for a nonlinear FDI. Second order SMOs have been suggested for filtering unwanted high frequencies due to un-modeled dynamics.[8-10]

In this paper, a second order nonlinear sliding mode observer is applied to detect CMG faults. The chattering in the conventional sliding observer is avoided by using the continuous observer law, and its convergence is proved. The magnitude of the oscillating disturbance is estimated properly. Contrary to reaction wheel cases,[4,9] consideration needs to be given to gimbal direction changes when isolating faults in satellites with CMGs. First, the sliding mode observer is considered for the detection of external disturbances. Next, the observing method is applied for the

[*] Professor, Dept. of Aero&Mech Eng, Korea Aerospace University, Goyang, KOREA, email:hsoh@kau.ac.kr
[†] Ph.D. Candi., Dept. of Aero&Mech Eng, Korea Aerospace University, Goyang, KOREA, e-mail:jimoony@kau.ac.kr

detection of internal disturbances induced by the CMG faults – both speed error faults and static/dynamic imbalance faults. Isolation schemes in the single fault cases are also shown.

ATTITUDE CONTROL WITH CMGS

The motion of a satellite with n-single gimbal CMGs is governed by the following equations:

$$\begin{aligned} I\dot{\omega} + \omega^{\times} I\omega + \omega^{\times} h &= u_C + u_S + u_I + u_E \\ D\dot{\sigma} &= -u_C \\ \dot{h} &= A\tau = -u_S \end{aligned} \tag{1}$$

where ω is the satellite angular velocity. Vector u_C is the control torque generated by steering the CMG's gimbal angle σ. The output torque matrix D is composed of the output torque vectors of d_i as $D = [d_1 \quad d_2 \quad \ldots \quad d_n]$ and changes with σ. The internal disturbances due to wheel fault are composed of u_S, the wheel speed error disturbance, and u_I, the wheel imbalance disturbance. The wheel momentum h is normally assumed fixed, and then $u_S = 0$. However, the wheel momentum can be disturbed by a speed fluctuation in the wheel fault, in which case u_S would have a nonzero value greater than the threshold. The matrix A is the gimbal configuration matrix composed of the wheel axis vectors of a_i's as $A = [a_1 \quad a_2 \quad .... \quad a_n]$. The vector u_E is the external disturbance torque from the sources outside of the satellite. Four CMGs are considered in this study. They are installed in a pyramid configuration, as shown in Figure 1.

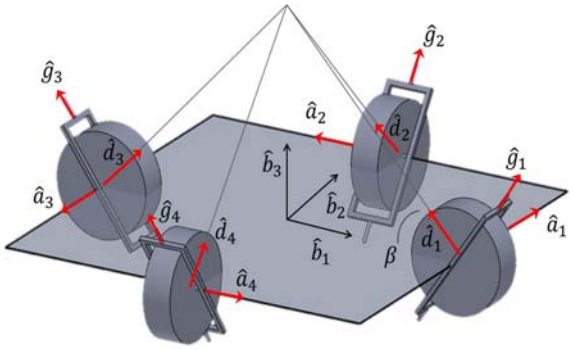

Figure 1. Pyramid Configured Installation of CMGs on a Satellite

DISTURBANCE OBSERVER DESIGN

When a disturbance, either internal or external, is exerted on the satellite body, the satellite attitude is then affected immediately. As a monitoring tool of the fault, a state observer can be used as a residual generator. Since the attitude equations are nonlinear, a nonlinear sliding observer is considered here as

$$I\dot{\hat{\omega}} + \hat{\omega}^{\times} I\hat{\omega} + \hat{\omega}^{\times} h = u_C - Iv \tag{2}$$

where $\hat{\omega}$ is the estimate of ω and v is the observer switching vector to be designed.

If the state estimate error is defined as $e = \omega - \hat{\omega}$, then

$$\dot{e} = f + I^{-1}u_D + v \tag{3}$$

where f is the system error due to e. Here u_D is either the speed error disturbance u_S or the imbalance disturbance u_I or any kind of the external disturbance u_E. The switching term v is designed by the second order sliding mode.[8-10] Let S be a sliding surface satisfying

$$\ddot{S} + z_o\dot{S} = \dot{e} + ce \tag{4}$$

where z_o and c are gains making $S \to 0$. Consider a Lyapunov candidate V as

$$V \equiv \frac{1}{2}(\dot{S}^T\dot{S} + S^T lS) \tag{5}$$

By choosing v as

$$v = z_o\dot{S} - ce - lS - d\,\mathrm{sgn}(\dot{S}) \tag{6}$$

then $\dot{V} \le 0$ and $S, e \to 0$ with the selection of a proper large gain d.[8-10] However, since the existence of chattering around the $S = 0$ surface can occur in this type of algorithm, the function $sat(\dot{S})$ has been occasionally used instead of $\mathrm{sgn}(\dot{S})$. In this paper, however, we propose to use a different continuous term instead of $sat(\dot{S})$ and consider its performance.

***Fact*)** With a sufficiently large gain d, switching the law $v = z_o\dot{S} - ce - lS - d\dot{S}$ stabilizes the observer at $e = 0$, and the disturbance is identified.

***pf*)** With the above v, $\dot{V}$ becomes

$$\dot{V} = \dot{S}^T[f + I^{-1}u_D - d\dot{S}] \le \left\|\dot{S}\right\|\left\|f + I^{-1}u_D\right\| - d\left\|\dot{S}\right\|^2 \tag{7}$$

Then $\dot{V} \le 0$ until $\left\|\dot{S}\right\| \ge \left\|f + I^{-1}u_D\right\|$ and $V \le V_U$. That is, V and $\dot{S}$ are bounded narrowly with a small initial S_o, then $e \to 0$. Finally, the estimate of disturbance $\hat{u}_D \to -I(f + v)$ □

Next, we consider the application of the above continuous observer on the detection and identification of external disturbances.

EXTERNAL DISTURBANCE DETECTION

Secular Disturbances

In orbit, a satellite occasionally experiences secular disturbance torque such as gravity gradient torque, solar pressure, and so on. This induces the wheel momentum to increase and finally causes saturation.[1] The detection of secular disturbances is thus necessary in real time to allow for proper remedies to be enacted. The observer designed above can be used as a detector of this type of disturbance. Assume a constant disturbance $u = [0.1 \quad 0 \quad 0]$ acts on the x-axis of a satellite during time $t = (20, 60)$ sec, as in Figure 2(c).

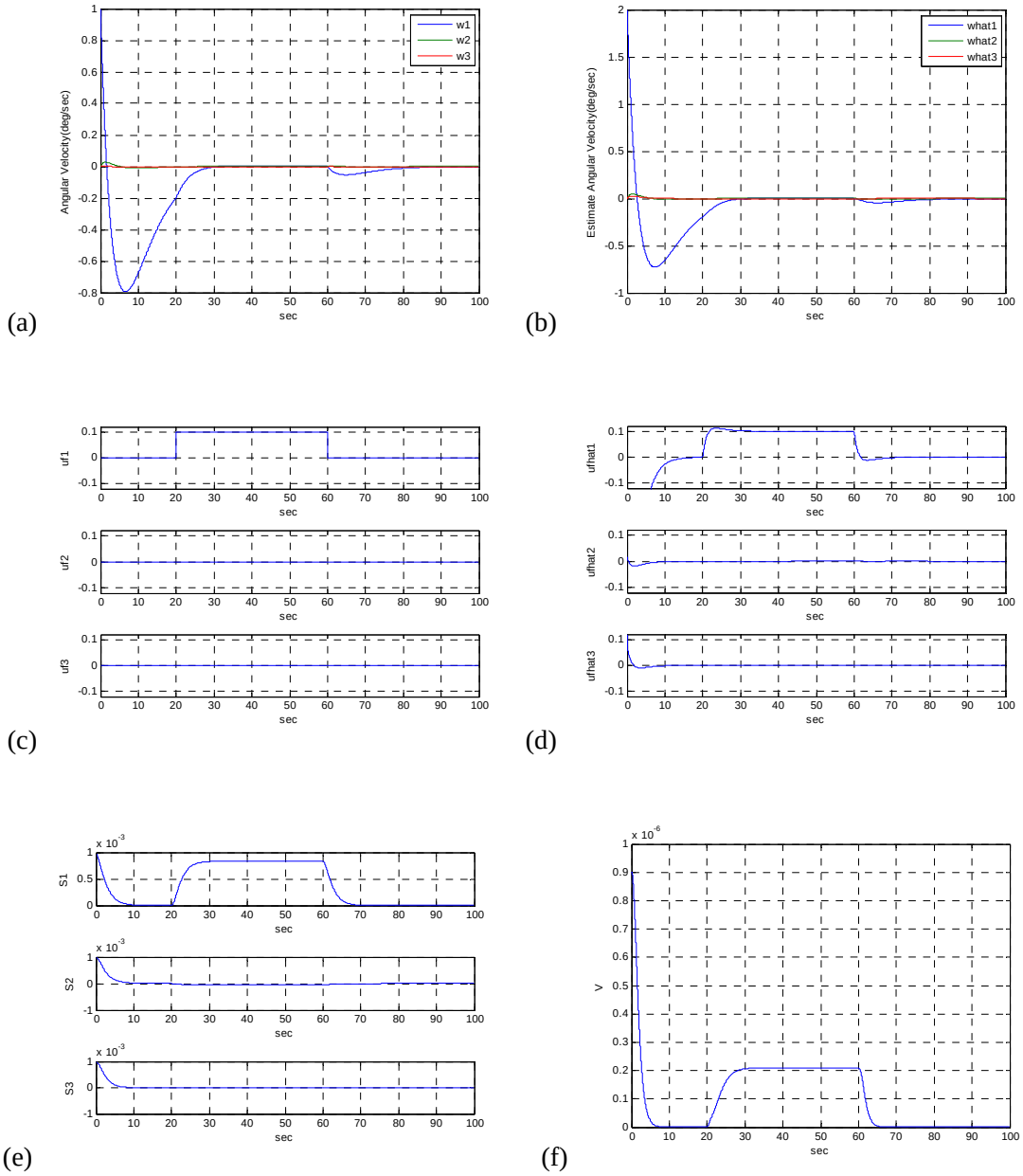

Figure 2. Observer Responses to Secular Disturbance

The angular velocity estimate $\hat{\omega}$ in Figure 2 (b) obtained from the observer aptly follows the real angular velocity ω in (a) even with a large initial error. By using the switching term, the disturbance is detected immediately at $t = 20$ sec, and the magnitude is also identified exactly in (d). The Lyapunov function $\dot{V} \to 0$, as shown in (f), and the sliding surface state $\dot{S} \to 0$ in (e) despite the existence of the disturbance as expected. Conclusively, the designed observer works well as a secular disturbance detector.

Oscillating Disturbances

As a satellite rotates around the Earth, it might be affected by oscillating disturbances due to aerodynamic forces, the Earth's oblate shape, or other factors. For precision attitude control, oscillating disturbances need to be detected. The ability to detect an oscillating disturbance depends on the observer processing rate. For the detection of a high frequency disturbance, the observer processing rate should be five to ten times greater than the disturbance frequency for a more precise prediction. Assume that the oscillating disturbance $u = [0.1\sin 2\pi f_D t \quad 0 \quad 0]$ acts on the satellite during time $t = (20, 60)$ sec on the y-axis. Here, the external disturbance frequency $f_D = 5$ Hz, and the observer is then set to process every 0.02 sec, i.e., 10 times faster than the disturbance frequency. The time constant of error e should then be reduced by using a bigger gain c. As shown in Figure 3 below, the oscillating disturbance in (a) is aptly detected and the magnitude is estimated exactly as in (b).

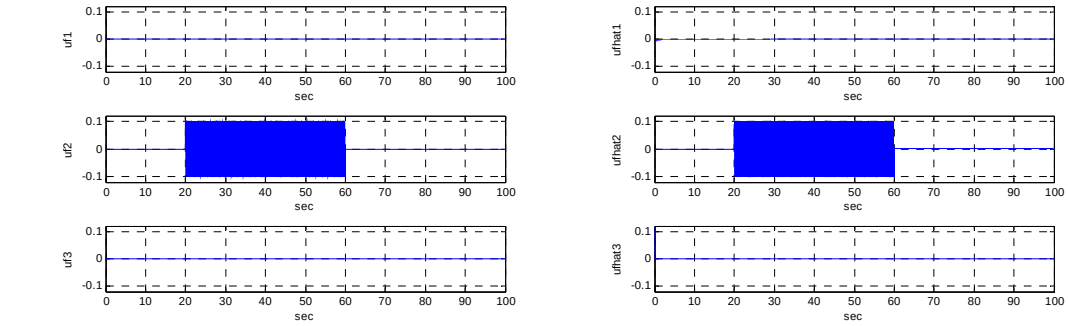

Figure 3. Observer Responses to an Oscillating Disturbance

Frequency Compensation for High Frequency Disturbances

Even when the disturbance frequency is much higher, the observer is still able to "detect" the disturbance on time, but the magnitude of the disturbance cannot be exactly identified in the case of a big time constant of the observer. For the exact estimation of the high frequency disturbance magnitude, we need a big gain c for a small time constant and high processing rate. However, there are limits with respect to practical satellite applications. Consider a case in which the disturbance of magnitude $u_D = 0.1$, and the frequency $f_D = 50$ Hz is exerted on the satellite, but the processor frequency and gain c remain fixed as in the previous secular disturbance. We can then detect the oscillating disturbance on time, but the magnitude is estimated to be much smaller than the real disturbance, as shown in Figure 4(a). In the case in which the disturbance frequency is much higher than the observer processor rate capacity, we need to rectify this problem with a proper method. Applying the frequency compensation method suggested in Reference 11 can be considered here. Without increasing the processor rate or gain c, the magnitude estimates are obtained by adapting the compensation as follows:

$$\hat{u}_{DC} = \hat{u}_D \sqrt{(\frac{2\pi f_D}{c})^2 + 1} = [-I(f + v)] \sqrt{(\frac{2\pi f_D}{c})^2 + 1} \tag{8}$$

Normally, the disturbance frequency f_D can be obtained from an observer output and can then be used in the above algorithm. When the compensation logic is applied as above, then the magnitude

of the disturbance can be identified with much closer proximity to the real value than the case in which the compensation logic is absent. This is visible in Figure 4(b).

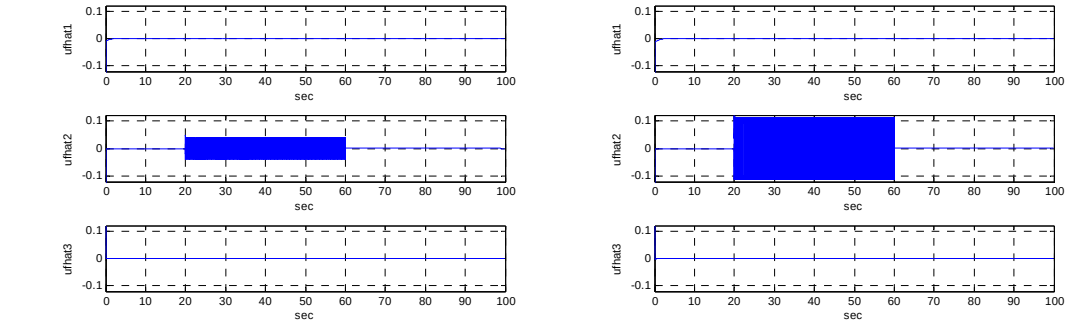

(a) (b)

Figure 4. Compensation Effects on an Oscillating Disturbance

ACTUATOR FAULT DETECTION AND ISOLATION

Internal Disturbances due to Wheel Speed Faults

CMG wheels rotate normally at a constant speed. The required torque for maneuvers are generated by steering the gimbals. Sustaining a constant wheel speed is thus important for precision satellite control. However, when a malfunction occurs in the speed controller, then the wheel speed might fluctuate and attitude quality degradation can occur. By immediately detecting the severity of wheel speed fluctuation, a proper remedy can be performed. The disturbance observer shown in the previous section can be used as an internal fault detector.

Assume that wheel No.1 in Figure 1 malfunctions during the maneuver time $t = (20, 60)$ sec interval, as shown in Figure 5(c). Even though the wheel speed fluctuates and thus generates oscillating disturbance torque, the satellite attitude is finally stabilized with some degradation, as shown in Figure 5(a). Different from the case in which the external torque was exerted on the single axis, the wheel induced disturbance torque is propagated to the all three axes, as shown in Figure 5(d). This is due to the change of CMG gimbal angles during maneuvers, as shown in Figure 5(b). The satellite operator needs to isolate the abnormal wheel from the normal wheels.

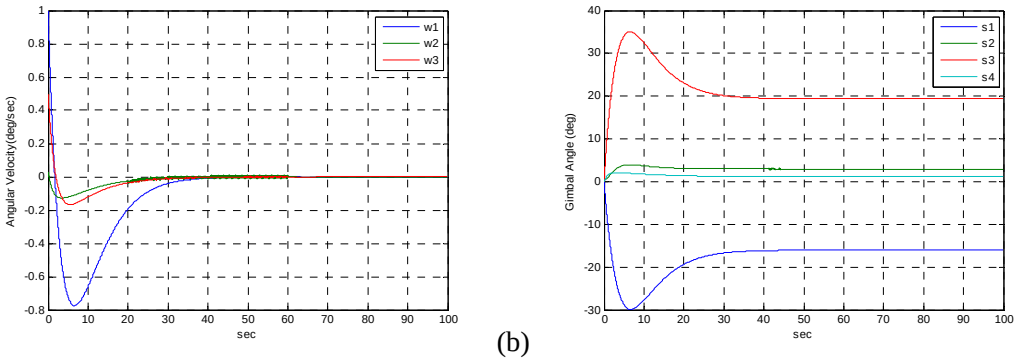

(a) (b)

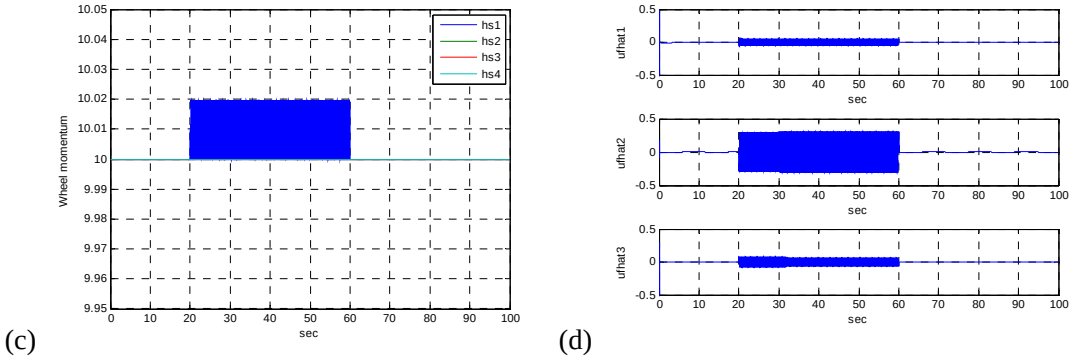

(c) (d)

Figure 5. Speed Fault in Wheel No.1 and Its Effects on the Maneuver

The disturbance effects on the satellite body depend on the gimbal configuration as $u_D = A\tau$. When the body disturbance estimate $\hat{u}_D$ is obtained, the possible candidate for the malfunctioning wheel can be chosen by multiplying A^T on u_D as

$$\hat{\tau} = A^T \hat{u}_D \tag{9}$$

We can then refine candidate responses, as shown in Figure 6(a). However, ambiguity still exists with respect to which wheel – No.1 or No.3 – is malfunctioning. However, by choosing the wheel axis with the direction nearest to $\hat{u}_D$, we can finally isolate No.1 as the fault wheel, as shown in Figure 6(b).

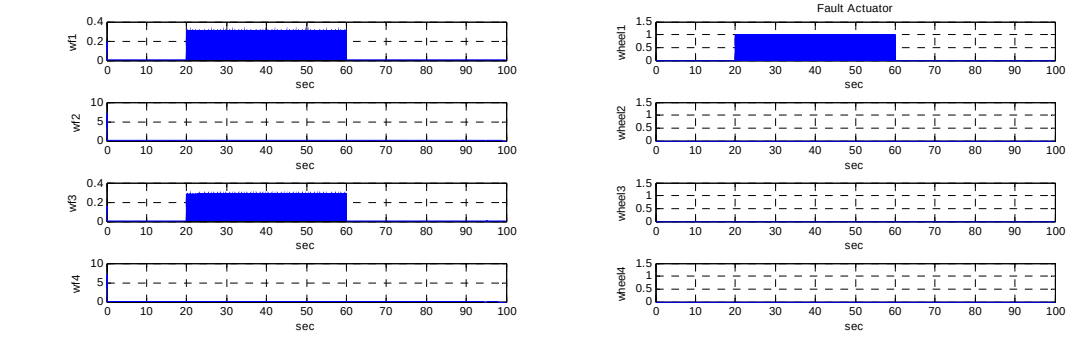

(a) (b)

Figure 6. Isolation of Wheel Speed Error Fault

Internal Disturbances due to Wheel Static Imbalance Faults

CMG wheels rotate at high speed to maintain their high angular momentum. Even a small imbalance in a wheel produces oscillating disturbances, which degrade the attitude quality.[2-4,11] Thus, balancing the wheels is necessary during the wheel manufacturing stage, and only well-balanced wheels are equipped in satellites. However, during the in-orbit mission period, wheel balance can be disrupted for several reasons, including loose rotor magneto bonding, bearing wear, and misalignment. This induces static and/or dynamic disturbances.[11] A static imbalance generates oscillating centrifugal force F as

$$F_i = U_s \Omega^2 \sin(\Omega t + \alpha) \tag{10}$$

where U_S is the static imbalance ($kg \cdot m$) and Ω is the wheel spin speed. The disturbance force induces the disturbance torque with respect to the satellite center of mass as

$$u_I = r_i \times F_i \tag{11}$$

where r_i is the position vector of the malfunctioning wheel. Assume that the wheel No.1 in Figure 1 has abrupt increase in its static imbalance due to a wheel malfunction during the maneuver time $t = (20, 60)$ sec interval. This imbalance induces the disturbance torque on the satellite body, as in Figure 7(a), and the disturbance torque is estimated by using the observer, as shown in Figure 7(b). (Here, in order to increase the simulation speed, we don't use the compensation filter.)

Since the x-axis torque is shown as zero, it is anticipated that either the No.1 or No.3 wheel has malfunctioned. We need a further step to isolate the malfunctioning wheel among the two candidate wheels. The static disturbance force can be derived using the formula

$$F_i = \frac{u_D \times a_i}{a_i \bullet r_i} \quad \text{where } a_i \bullet r_i \neq 0 \tag{12}$$

By checking whether or not F_i is orthogonal to the i-th wheel axis a_i, we can identify the malfunctioning wheel. As shown in Figure 7(c), F_i is orthogonal to the wheel axis a_1 in the No.1 frame, but not to the wheel axis a_3 in Figure 7(d). Thus, we can conclude the No.1 wheel has malfunctioned. When $a_i \bullet r_i = 0$ at that instant, however, the magnitude F_i is un-determined.

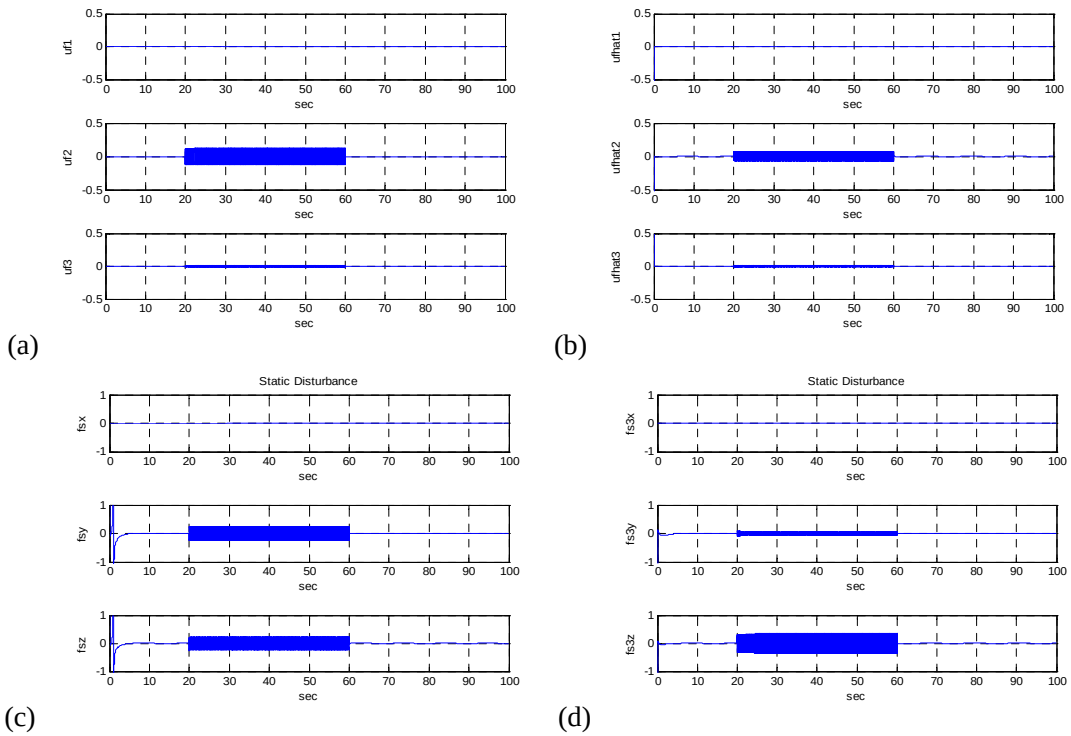

Figure 7. Isolation of Static Imbalance Fault Wheel

Internal Disturbances due to Wheel Dynamic Imbalance Faults

A dynamic imbalance generates oscillating disturbance torque T_i as

$$T_i = U_d \Omega^2 \sin(\Omega t + \alpha) \tag{13}$$

where U_d is the dynamic imbalance ($kg \cdot m^2$) and Ω is the wheel spin speed. The fact that the dynamic disturbance torque is orthogonal to the spin axis of the wheel when it malfunctions can be used as the criteria to isolate the fault wheel from the normal wheels. By checking the orthogonality of $\hat{u}_D$ with respect to each wheel spin axis at an instant, we can identify the fault wheel. Assume that the dynamic balance of wheel No.1 is disrupted during the maneuver time $t = (20, 60)$ sec for some reason. The disturbance estimate $\hat{u}_D$ is obtained by the disturbance observer, and the resolved components of $\hat{u}_D$ on each CMG gimbal frame are monitored. As depicted in Figure 8, the spin axis component in CMG No.1 is zero, but the one in the other CMGs (here, CMG No.3) is non-zero. Thus, we can conclude the malfunction has occurred in CMG No.1.

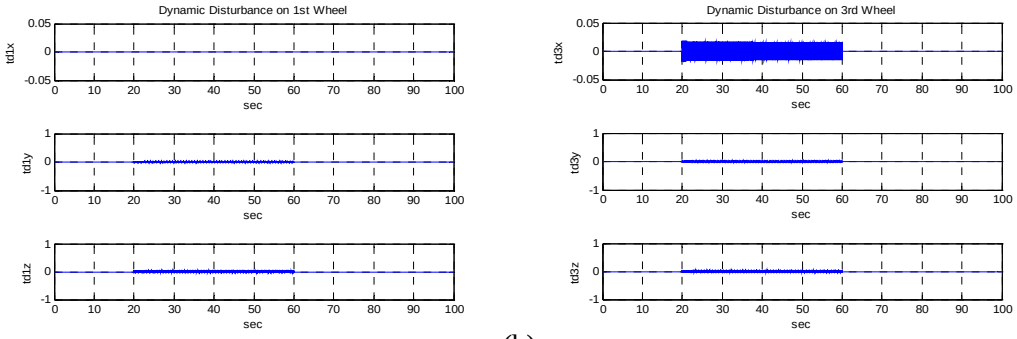

(a) (b)

Figure 8. Isolation of Dynamic Imbalance Fault Wheel

Table 1 conclusively summarizes the fault scenario of the three fault cases in the CMG wheels. The directions of the estimated disturbances $\hat{u}_D$ and $\hat{F}$ are considered with respect to whether they are orthogonal or parallel to each wheel spin axis a_i and the CMG location vector r_i. With proper programming, this table can be used for fault detection in supervisory software.

Table 1. CMG Single Fault Scenario Isolation Criteria

Fault Type	$\hat{u}_D \times a_i$	$\hat{u}_D \cdot r_i$	$\hat{F} \cdot a_i$	$\hat{u}_D \cdot a_i$
Wheel Speed Fault	0			
Static Imbalance Fault	**0***	0	0	
Dynamic Imbalance Fault				0

*) instantaneous case only.

CONCLUSION

A newly revised continuous nonlinear second order sliding mode observer is suggested and applied with a convergence proof for disturbance detection for satellites with CMGs. Both secular and oscillating external disturbances are aptly detected, and the magnitude is identified successively. Even the highly oscillating disturbance can be effectively identified using the suggested frequency compensation algorithm. Internal wheel faults that result from speed errors and static/dynamic imbalances can be detected using the suggested observer and isolated by applying the proper identifying logics.

ACKNOWLEDGEMENTS

This work was supported by the National Space Lab Program 2013 in Korea.

REFERENCES

1. M. Sidi, *Spacecraft Dynamics and Control*, Cambridge University Press, 1997.
2. R. Masterson et al, “Development and validation of reaction wheel disturbance models: empirical model,” Journal of Sound and Vibration, Vol. 249, No. 3, pp. 575-598, 2002.
3. S. Taniwaki and Y. Ohkami, “Experimental and Numerical Analysis of Reaction Wheel Disturbance,” JSME International Journal, Vol. 46, No.2, 2003.
4. H. Oh et al, “Torque and force measurement of a prototype KAU reaction wheel and the effect of disturbance on the attitude stability of spacecraft,” Journal of Mechanical Science and technology, Vol. 15, No. 6, pp. 743-751, 2001.
5. V. Venkatasubramanian et al, “A review of process fault detection and diagnosis Part I; Quantitative model based methods,” Computers and Chemical Engineering, Vol. 27, pp. 293-311, 2003.
6. R, Chen, et al, “Health monitoring of a satellite system,” Journal of Guidance, Control and Dynamics, Vol. 29, No. 3, 2006.
7. B. Ahmadi and M. Namvar, “Robust detection and isollation of failures in satellitte attitude sensors and gyro,” Robotica, Vol. 30, 2012.
8. W. Chen and M. Saif, “Robust fault detection in uncertain nonlinear systems via a second order slding mode observer,” Proceedings of the 40th IEEE Conference on decision and control, Orlando, Fl., U.S.A., 2001.
9. T. Jiang and K. Khorasani, “Fault detection, isolation, and reconstruction strategy for a satellite’s attitude control subsystem with redundant wheels,” IEEE, 2007.
10. J. Slotine and W. Li, *Applied Nonlinear Control*, Prentice Hall, 1991.
11. H. Oh and D. Cheon, “Precision measurements of reaction wheel disturbances with frequency compensation process,” Journal of Mechanical Science and Technology, Vol. 19, No. 1, pp. 136-143, 2005.